*Astronomical and Astrophysical Transactions* (*AApTr*), 2026, Vol. 36, Issue 1, pp. 31–36,
ISSN 1055-6796, Photocopying permitted by license only, ©Cambridge Scientific Publishers

# Modeling the dynamic evolution of the Emilkowalski asteroid family based on constructed formation scenario

E.D. Kuznetsov*, A.S. Perminov, V.S. Safronova

*Ural Federal University, 51 Lenina Avenue, Yekaterinburg, 620000 Russia*

*Received 7 December, 2025; accepted 10 December, 2025*

This paper tests a previously constructed scenario for the formation of the Emilkowalski asteroid family. We model the orbital evolution of this young family from the past to the present using a cascade-decay model based on simulations of probabilistic evolution. The obtained solution represents a zero-order approximation of the Emilkowalski family's formation scenario. It reproduces the observed distribution of semi-major axes within the family and qualitatively matches the distributions of orbital eccentricities and inclinations.

*Keywords*: Emilkowalski family, family formation scenario, cascade decay, orbital evolution, numerical modeling

## 1 Introduction

The young Emilkowalski asteroid family is located in the central part of the Main Belt (semi-major axis $a = 2.60$ AU, eccentricity $e = 0.15$, inclination $I = 17.75°$). The family was discovered in 2006 as a group of three asteroids (Nesvorny and Vokrouhlicky, 2006). Later, the number of identified members increased to nine (Pravec et al., 2018; Fatka et al., 2020). The largest member, asteroid (14627) Emilkowalski, was classified as a D-type based on photometric observations (Pravec et al., 2018).

In Kuznetsov et al. (2025a), four additional members of the family were identified. A list of all 13 currently known family members and their proper orbital elements is provided in Perminov (2024, Table A4). In Kuznetsov et al. (2025b), a preliminary scenario for the formation of the Emilkowalski family was constructed based on the dynamical evolution of the nominal orbits. This preliminary scenario was later refined in Kuznetsov et al. (2025c) using the results of probabilistic orbital evolution modeling.

In the present work, we model the dynamical evolution of the Emilkowalski asteroid family from the past to the present in order to verify the correctness of the proposed formation scenario.

*Email: eduard.kuznetsov@urfu.ru

## 2 Methods

The dynamical evolution of the Emilkowalski family was modeled using the Orbit9 program, which is part of the OrbFit[1] software package (Orbfit Consortium, 2011). The model includes perturbations from the eight major planets and Pluto, the oblateness of the Sun, relativistic corrections, as well as the Yarkovsky and YORP effects.

Kuznetsov et al. (2025c) considered the dynamical evolution of 250 orbital clones for each asteroid in the family. Based on the obtained results, a scenario of cascade destruction of the parent body was constructed (Figure 1). The parent bodies of each pair are shown in gray; for each parent asteroid, the median age of pair formation (in kyr) is marked in red.

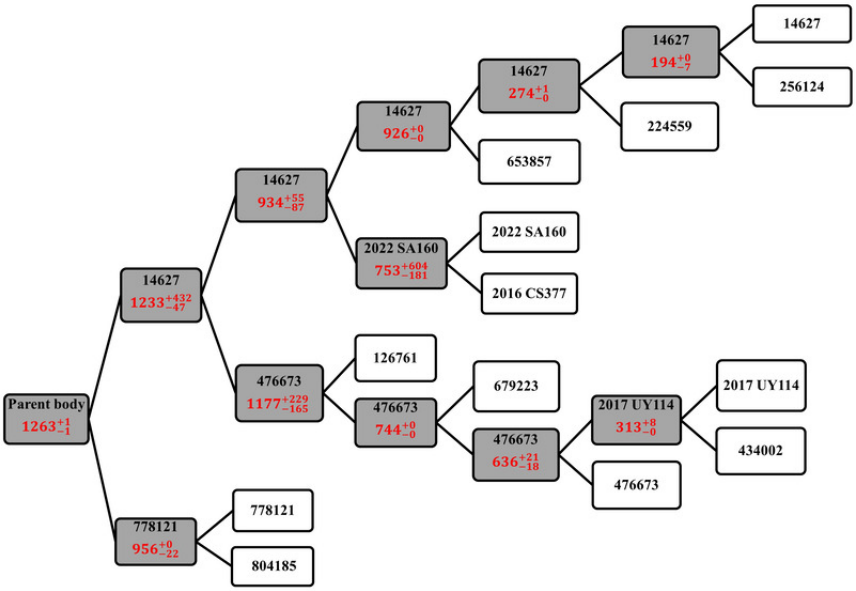



**Figure 1** Scenario of the formation of the Emilkowalski asteroid family.

When modeling the breakup of the parent body, we do not consider the physical mechanisms leading to fragmentation. This requires a separate study. Possible causes include catastrophic or cratering collisions, rotational breakup, disruption of a contact binary, or breakup of a binary under tidal forces or the BYORP effect. As initial conditions, we consider the dynamical state of the system at the moment just before breakup.

The initial conditions for the modeling of each asteroid and parent body were determined as follows. The first breakup of the parent body into asteroids (14627) Emilkowalski and (778121) 2009 VF107 occurred 1263 kyr ago. At that moment, the mass of (778121) 2009 VF107 included the mass of (804185) 2015 WH29, and the mass of (14627) Emilkowalski included the masses of all other family members. The nominal orbit of (14627) Emilkowalski at 1263 kyr ago was taken as the initial orbit for modeling the evolution of the pair.

[1] http://adams.dm.unipi.it/orbfit/

At that moment, the coordinates and velocities of (14627) Emilkowalski were used as the center-of-mass state vector of the two daughter bodies. Assuming that the mutual distance between the daughter bodies equaled the Hill radius of the larger body and their relative velocity equaled its escape velocity, we obtained the initial coordinates and velocities of the daughter bodies.

A set of eight initial configurations for the daughter bodies was generated:

1. Two positions along the heliocentric radius vector of the parent body – one closer to the Sun, one farther away, and vice versa.
2. Two positions along a line perpendicular to this heliocentric radius vector.
3. For each spatial configuration, two opposite directions of the relative velocity.

We model the orbital evolution of the daughter bodies until their subsequent breakup. For the parent body, the modeling spans 30 kyr for (14627) Emilkowalski (from 1263 to 1233 kyr ago) and 307 kyr for (778121) 2009 VF107 (from 1263 to 956 kyr ago).

To account for the Yarkovsky and YORP effects, we assume typical D-type asteroid parameters (Ribeiro et al., 2023): density $\rho = 1300$ kg m$^{-3}$, thermal conductivity $k = 0.5$ W m$^{-1}$ K$^{-1}$, heat capacity $c = 500$ J kg$^{-1}$ K$^{-1}$, and thermal emission and absorption coefficients $\alpha = \beta = 1$. Diameters $D$ were adopted from Kuznetsov et al. (2025b, Table 1). We use three values of spin-axis tilt: 0°, 90°, and 180°, and four rotation periods: $3^h$, $6^h$, $9^h$, and $12^h$.

Thus, 96 clones of each orbit were generated (8 initial positions × 3 tilt angles × 4 rotation periods).

After integrating the 96 clones, we selected the orbit with the smallest Kholshevnikov metric $\rho_2$ (Kholshevnikov et al., 2016) relative to the nominal orbit (obtained by integrating backward from epoch MJD 60800). This orbit was then used as the basis for constructing the next breakup, generating another set of 96 clones, and continuing the modeling up to epoch MJD 60800.

## 3 Results

Table 1 shows, for each breakup time $T$, the effective diameter of the larger body in the pair, the positional orbital elements $a_n$, $e_n$, $I_n$ of the nominal orbit, and the ranges $[a_{\min}, a_{\max}]$, $[e_{\min}, e_{\max}]$, and $[I_{\min}, I_{\max}]$ of the 96 clones.

When the modeling reached the present epoch, each asteroid had 96 final orbital clones. These were compared with the current (nominal) orbital elements of the Emilkowalski family.

Table 2 shows the final ranges of $a$, $e$, and $I$ for the clones, together with the current nominal orbital elements.

Over the entire modeling interval, the semi-major axes of all asteroids stay close to their expected nominal values. For about 120 kyr following the parent-body breakup, the orbital eccentricities and inclinations also remain close to nominal values (Table 1). At later times, their deviations increase, likely due to different secular evolution rates of the clones relative to the nominal orbit.

**Table 1** Orbital elements and asteroid diameters at the breakup moments.

| $T$, kyr | $D$, m | $a_n$, AU | $[a_{\min}, a_{\max}]$, AU | $e_n$ | $[e_{\min}, e_{\max}]$ | $I_n$, ° | $[I_{\min}, I_{\max}]$, ° |
|---|---|---|---|---|---|---|---|
| **(14627) Emilkowalski** | | | | | | | |
| 1233 | 7372 | 2.5995 | 2.5981, 2.5996 | 0.2807 | 0.2782, 0.2813 | 17.402 | 17.373, 17.408 |
| 934 | 7334 | 2.5983 | 2.5978, 2.6006 | 0.1808 | 0.1606, 0.1648 | 16.779 | 16.963, 17.017 |
| 926 | 7291 | 2.5990 | 2.5999, 2.6005 | 0.1930 | 0.1727, 0.1728 | 15.790 | 16.396, 16.402 |
| 274 | 7254 | 2.5989 | 2.5982, 2.6012 | 0.2341 | 0.1649, 0.1662 | 18.576 | 18.913, 18.991 |
| 194 | 7105 | 2.6001 | 2.5982, 2.6002 | 0.1450 | 0.1900, 0.1907 | 17.347 | 18.334, 18.381 |
| **(476673) 2008 TN44** | | | | | | | |
| 1177 | 3007 | 2.6017 | 2.5965, 2.6002 | 0.1978 | 0.1924, 0.1922 | 17.118 | 17.177, 17.230 |
| 744 | 2478 | 2.5978 | 2.5957, 2.5998 | 0.2406 | 0.1877, 0.1947 | 16.452 | 16.854, 16.942 |
| 636 | 2279 | 2.5987 | 2.5959, 2.5992 | 0.1569 | 0.1882, 0.1907 | 16.493 | 16.220, 16.273 |
| 313 | 1500 | 2.6010 | 2.5950, 2.5991 | 0.2772 | 0.1131, 0.1179 | 14.171 | 17.316, 17.427 |
| **(778121) 2009 VF107** | | | | | | | |
| 956 | 2497 | 2.6014 | 2.5961, 2.6015 | 0.1916 | 0.1553, 0.1651 | 14.908 | 15.236, 15.357 |
| **2022 SA160** | | | | | | | |
| 753 | 1829 | 2.6011 | 2.5964, 2.6015 | 0.2648 | 0.2168, 0.2216 | 18.527 | 19.695, 19.770 |

**Table 2** Final ranges of orbital elements of clones and nominal orbital elements at epoch MJD 60800.

| Asteroid | $a_0$, AU | $[a_{\min}, a_{\max}]$, AU | $e_0$ | $[e_{\min}, e_{\max}]$ | $I_0$, ° | $[I_{\min}, I_{\max}]$, ° |
|---|---|---|---|---|---|---|
| 14627 | 2.59928 | 2.59751, 2.60025 | 0.1495 | 0.1023, 0.1043 | 17.752 | 17.106, 17.165 |
| 126761 | 2.59974 | 2.59527, 2.59981 | 0.1511 | 0.1081, 0.1177 | 17.713 | 17.283, 17.417 |
| 224559 | 2.60003 | 2.59669, 2.60243 | 0.1493 | 0.1026, 0.1048 | 17.725 | 17.110, 17.189 |
| 256124 | 2.60022 | 2.59628, 2.60110 | 0.1481 | 0.1027, 0.1048 | 17.769 | 17.091, 17.199 |
| 434002 | 2.59938 | 2.59447, 2.59930 | 0.1558 | 0.1879, 0.1944 | 17.533 | 18.868, 18.948 |
| 476673 | 2.59871 | 2.59504, 2.59914 | 0.1567 | 0.1131, 0.1179 | 17.472 | 17.316, 17.427 |
| 653857 | 2.60114 | 2.59537, 2.60322 | 0.1524 | 0.1022, 0.1142 | 17.556 | 16.536, 17.426 |
| 679223 | 2.60043 | 2.59530, 2.59958 | 0.1462 | 0.1137, 0.1179 | 17.750 | 17.333, 17.411 |
| 778121 | 2.60046 | 2.59586, 2.60001 | 0.1531 | 0.1041, 0.1085 | 17.506 | 17.144, 17.297 |
| 804185 | 2.59917 | 2.59609, 2.59999 | 0.1480 | 0.1047, 0.1076 | 17.766 | 17.167, 17.270 |
| 2016 CS377 | 2.60046 | 2.59567, 2.59981 | 0.1492 | 0.1039, 0.1068 | 17.640 | 17.188, 17.288 |
| 2017 UY114 | 2.59918 | 2.59429, 2.59953 | 0.1533 | 0.1869, 0.1952 | 17.604 | 18.855, 18.956 |
| 2022 SA160 | 2.60093 | 2.59562, 2.59962 | 0.1527 | 0.1039, 0.1069 | 17.517 | 17.187, 17.284 |

We compared the final orbital elements of all clones with the current nominal values. For all asteroids except (679223) 2018 VB69, the nominal semi-major axis deviates from the mean of the interval $[a_{\min}, a_{\max}]$ by less than $3\sigma$, where $\sigma$ is the standard deviation (Table 3). Figure 2 shows the deviations $\Delta$ in units of $\sigma$.

The standard deviations for the eccentricities and inclinations are too large to be informative, so they are not presented here.

**Table 3** Standard deviations of the semi-major axes for the Emilkowalski family.

| Asteroid | $\sigma$, AU |
|---|---|
| 14627 | 0.00068 |
| 126761 | 0.00112 |
| 224559 | 0.00138 |
| 256124 | 0.00047 |
| 434002 | 0.00170 |
| 476673 | 0.00068 |
| 653857 | 0.00133 |
| 679223 | 0.00084 |
| 778121 | 0.00135 |
| 804185 | 0.00143 |
| 2016 CS377 | 0.00164 |
| 2017 UY114 | 0.00088 |
| 2022 SA160 | 0.00207 |

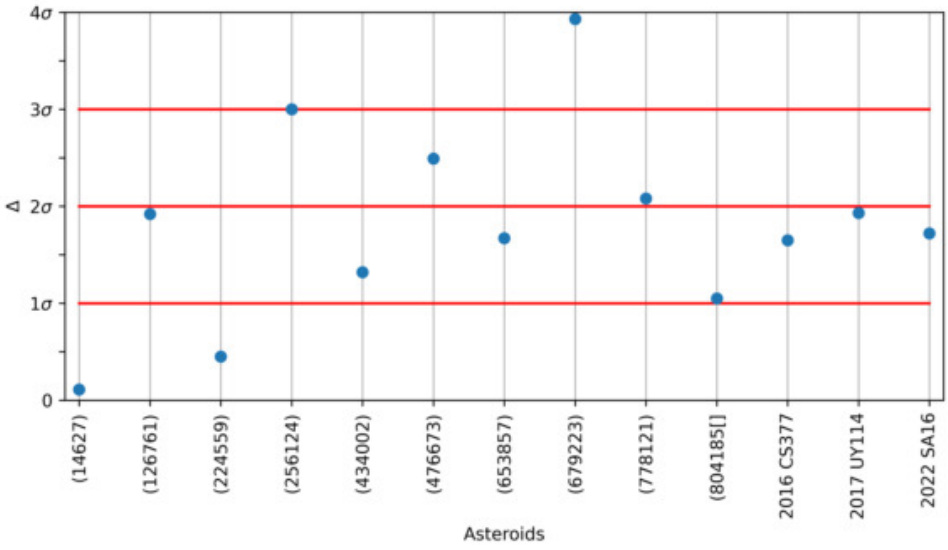



**Figure 2** Deviations $\Delta$ of the nominal semi-major axes from the mean values of $[a_{\min}, a_{\max}]$.

## 4 Conclusions

Modeling the dynamical evolution of the Emilkowalski asteroid family from the past to the present shows that, for all asteroids except (679223) 2018 VB69, the final nominal semi-major axis deviates from the mean value of the clone range by no more than $3\sigma$.

For all asteroids except (434002) 2000 SM320 and 2017 UY114, the final eccentricities of the clones are smaller than the nominal values and lie around 0.11–0.12. For

these two asteroids, the clone inclinations are also higher than the nominal inclinations (exceeding 18°). For the remaining asteroids, the inclinations are slightly lower than the nominal ones but remain within the clone ranges (the absolute difference does not exceed 0.65°).

We conclude that the obtained solution provides a zero-order approximation of the Emilkowalski family formation scenario. It reproduces the observed distribution of semi-major axes and qualitatively matches the distributions of orbital eccentricities and inclinations. Future work will incorporate different pair-formation mechanisms to further improve the accuracy of the Emilkowalski family formation model.

## Funding

The study was funded by the Russian Science Foundation grant No. 24-22-00143, https://rscf.ru/en/project/24-22-00143/.

## References

Fatka P., Pravec P., Vokrouhlicky D. (2020) Icarus, 338, 113554, doi: 10.1016/j.icarus.2019.113554

Kholshevnikov K.V., Kokhirova G.I., Babadzhanov P.B., Khamroev U.H. (2016) MNRAS, 462, 2275–2283, doi: 10.1093/mnras/stw1712

Kuznetsov E.D., Vasileva M.A., Perminov A.S., Safronova V.S. (2025a) Sol. Syst. Res., 59, 8 doi: 10.1134/S0038094624601129

Kuznetsov E.D., Safronova V.S., Vasilyeva M.A., Perminov A.S. (2025b) Sol. Syst. Res., 59, 10, doi: 10.1134/S0038094624601403

Kuznetsov E.D., Perminov A.S., Safronova V.S. (2025c) Sol. Syst. Res., 59, 97, doi: 10.1134/S0038094625600660

Nesvorny D., Vokrouhlicky D. (2006) AJ 132, 5, 1950–1958, doi: 10.1086/507989

Perminov A. (2024) Mendeley Data, doi: 10.17632/hs4rtk9np9.2

Pravec P., Fatka P., Vokrouhlicky D., et al. (2018) Icarus, 304, 110–126, doi: 10.1016/j.icarus.2017.08.008

Ribeiro T.M., D'Ambrosio A., Calabuig G.J.D., et al. (2023) Acta Astronaut., 212, 213–225, doi: 10.1016/j.actaastro.2023.07.035